European Journal of Pharmaceutical Sciences 109 (2017) 372–380

Contents lists available at ScienceDirect

European Journal of Pharmaceutical Sciences

journal homepage: www.elsevier.com/locate/ejps

Effect of surfactants and drug load on physico-mechanical and dissolution properties of nanocrystalline tadalafil-loaded oral films

Parameswara Rao Vuddanda[a], Miguel Montenegro-Nicolini[b], Javier O. Morales[a,b,c], Sitaram Velaga[a,*]

[a] Pharmaceutical and Biomaterial Research Group, Division of Medical Sciences, Department of Health Sciences, Luleå University of Technology, Luleå 97187, Sweden
[b] Department of Pharmaceutical Sciences and Technology, University of Chile, Santiago 8380494, Chile
[c] Advanced Center for Chronic Diseases (ACCDiS), Santiago 8380494, Chile

ARTICLE INFO

Keywords:
Tadalafil
Oral films
Nanocrystals
HPMC
Vitamin E TPGS
Poloxamer
Surfactants

ABSTRACT

The aim of the present work was to prepare tadalafil (TDF) nanocrystals-loaded oral polymeric films (OFs) and investigate the effect of hydrophilic surfactants and drug loads on the physico-mechanical and dissolution properties. The nanosuspensions of TDF were prepared by high shear homogenization. HPMC based placebo casting film gel was prepared and mixed with TDF nanosuspensions. Films were casted using an automated film applicator and dried at 60 °C for 45 min. Particle size (PS), polydispersity index (PDI), and zeta potential (ZP) of TDF nanosuspensions were measured in a Zetasizer. The films were characterized using SEM, AFM, DSC, TGA and PXRD. The mechanical properties and in vitro drug release were determined using standard methods. TDF existed in crystalline form and the particles remained in the nano-range in redispersed films. TDF nanocrystals were embedded in the polymeric matrix and the drug loaded films were rough on the surface. Mechanical properties of the films varied with changes in drug load and surfactant. Significant changes in the disintegration times were noticed in films containing surfactants compared to surfactant-free films. About 80% of the drug release was observed between 3 and 30 min. TPGS showed better TDF release from the films at different drug loads.

Chemical compounds: Hydroxy propyl methyl cellulose (PubChem CID: 57503849); Glycerol (PubChem CID: 753); Pluronic F-68 (PubChem CID: 24751); Vitamin E TPGS (PubChem CID: 71406).

1. Introduction

Oral polymeric films (OFs), also known as oral strips and oral thin films could be considered as oromucosal preparations. They are relatively new and alternative dosage forms of conventional oral preparations (Dixit and Puthli, 2009; Hoffmann et al., 2011; Kathpalia and Gupte, 2013). They can be administered without water, and are disintegrated when placed on/or under the tongue. Subsequently, the drug is released from the film and the resulting solution/dispersion is swallowed. OFs are considered more patient-friendly dosage forms compared to other solid dosage forms such as tablets or capsules, and thus gained tremendous attention in the recent years (Bhosle et al., 2009). OFs can also be considered as a customized or personalized dosage form for a patients like pediatrics, geriatrics, bed-ridden and patients with different diseases such as oral and throat cancer, cardiovascular diseases, gastrointestinal problems, mental illness and CNS disorders (Alzheimer's and Parkinsonism) (Kathpalia and Gupte, 2013). Visser et al., has reported OFs as feasible extemporaneous preparations for individual pharmacotherapy (Visser et al., 2015b).

Different formulation excipients, processing strategies and characterization methods pertaining to the development of OFs have been reviewed elsewhere (Hoffmann et al., 2011; Preis et al., 2013). Briefly, OFs are comprised of film forming polymers (biodegradable and biocompatible), plasticizers, sweeteners, flavors and other excipients (e.g. buffers, stabilizers). They are prepared by conventional methods such as solvent casting, hot melt extrusion and rolling/compression. Recently, freeze drying, printing and electrospinning technologies have been investigated in the preparation of OFs (Buanz et al., 2011; Buanz et al., 2015; Illangakoon et al., 2014; Vuddanda et al., 2016). Standard techniques have been used to characterize physicochemical and morphological properties of films. In addition, mechanical properties (tensile strength, Young's modulus, etc.) of OFs are determined as they are important for handling, performance and stability.

At present, OFs technology is mainly used to formulate water

* Corresponding author at: Department of Health Sciences, Luleå University of Technology, Luleå, Sweden.
E-mail addresses: parameswara.rao.vuddanda@ltu.se (P.R. Vuddanda), miguel.montenegro@ug.uchile.cl (M. Montenegro-Nicolini), jomorales@ciq.uchile.cl (J.O. Morales), sitaram.velaga@ltu.se (S. Velaga).

http://dx.doi.org/10.1016/j.ejps.2017.08.019
Received 4 July 2017; Received in revised form 2 August 2017; Accepted 7 August 2017
Available online 18 August 2017

soluble active pharmaceutical ingredients (APIs). In these films, the drug is usually dissolved or dispersed in the polymeric matrix that facilitates wetting, improves apparent solubility or dissolution and stability. For instance, the marketed OFs of ondansetron and sildenafil citrate, where the drug is dispersed in polymers (PVA or HPMC) with other required excipients. However, over 40% of NCEs is poorly water soluble, i.e. BCS class II or IV, leading to inadequate bioavailability, posing major challenges in the formulation and drug delivery (Savjani et al., 2012).

In the recent years, film technology has been exploited to formulate the poorly soluble drugs. Film of poorly soluble drug like ibuprofen has been prepared where the drug is dispersed in polymers (chitosan). But recrystallization of these drugs (into micron size particles) was observed in post-preparation and storage due to poor impregnation of the drug at higher drug load (Tang et al., 2014). In another study, films of ibuprofen have been prepared using methanol/acetone mixtures resulting in a solid solution. The excessive organic solvent residual is a potential disadvantage with this approach. In addition, there is a risk of recrystallization of the drug that eventually leads to poor absorption or bioavailability.

Size reduction is the primary approach to improve dissolution rate of poorly soluble drugs. Nanocrystal technology is a widely accepted approach for enhancing bioavailability where the drug dissolution is the rate limiting step (Junghanns and Muller, 2008; Yousaf et al., 2015). In fact, several drug products based on this technology have been commercialized (Möschwitzer, 2013). The idea of incorporating nanocrystals of Biopharmaceutical Classification System (BCS) class II drugs into polymeric films (i.e. solid suspension-type of system) has been recently introduced by Sievens-Figueroa et al., and Krull et al., to enhance drug dissolution and bioavailability (Krull et al., 2016; Sievens-Figueroa et al., 2012). Furthermore, both surfactant-free and surfactant-based films were claimed to stabilize nanoparticles and enhance dissolution of different BCS class II drugs (Beck et al., 2013; Krull et al., 2015). However, these studies have not properly indicated that under what conditions whether surfactants should be used or not. In other study, the existence of different polymorphs of loperamide hydrochloride (a poorly water-soluble drug) when incorporated in suspended (nanoparticle) form into HPMC and HPC orodispersible films has been reported (Woertz and Kleinebudde, 2015). However, the effect of drug loading (in the form of nanocrystals) into polymeric films has not been extensively studied.

Tadalafil (TDF) (molecular weight 389.4 g/mol) is a selective phosphodiesterase (PDE5) inhibitor and is used in the treatment of erectile dysfunction (ED) and benign prostatic hyperplasia (Frajese et al., 2006). The dosage regimen for ED is in the range of 5–20 mg and the maximum plasma concentration (C_{max}) after oral administration of a 20 mg tablet is 378 μg/L. It is a white crystalline solid with aqueous solubility of 2.80 μg/mL. The value of logP and pKa is 2.48 and 16.68, respectively. Thus, TDF belongs to BCS class-II and its oral bioavailability has been claimed to be limited by solubility and dissolution rate (Mehanna et al., 2010; Park et al., 2014; Vyas et al., 2009). TDF solubility and bioavailability issues have been addressed by amorphous solid dispersion, inclusion complexation, cocrystallization and nanonization techniques (Badr-Eldin et al., 2008; Choi and Park, 2017; Obeidat and Sallam, 2014; Vinesh et al., 2013). Obeidat et al., has revealed that nanosupensions/crystals of TDF were able to enhance dissolution and can theoretically enhance oral bioavailability. However, TDF amorphous solid dispersions and nanodispersions (liquid system) are prone to instability. Hence, incorporating these nanocrystals into polymeric films could be a rational approach that may circumvent instability problems with amorphous solid dispersions while keeping improved solubility and dissolution of TDF.

The main aim of this work was to develop nanocrystal of TDF-loaded OFs. In addition, the effect of drug (nanocrystal)-load and surfactants on physico-mechanical and dissolution properties of OFs were investigated. HPMC was used as a film forming polymer, surfactants; Poloxamer 188 (pluronic F-68) and vitamin E TPGS at different concentrations were considered. TDF nanocrystal loads (or doses) of 10 and 20 mg in size of film (i.e. 6 cm^2 or 2 cm × 3 cm) was considered in this study.

2. Material

Tadalafil (European Pharmacopoeia quality) was provided by Phalanx Labs Pvt. Ltd., India as a gift sample. Hydroxy propyl methyl cellulose, 6cp (Pharmacoat 606) was received from Shin-Etsu, Japan. Poloxamer 188 (pluronic F-68) and D-α-Tocopherol polyethylene glycol 1000 succinate (vitamin E TPGS) NF grade were received as gift samples from BASF and Antares health products Inc., Germany, respectively. Glycerol and acesulfame potassium were purchased from VWR chemicals, Sweden. Fluoropolymer coated polyester film (Scotch pak release liner 1022) was received from 3M Inc., USA. Water used in all experiments was ultrapure collected freshly from a Millipore water system (Milli Q, Sweden). The other materials were purchased locally and used as such in this work.

3. Methods

3.1. Preparation of nanocrystal suspensions

The nanocrystal suspension was prepared by the high shear homogenization method. The required quantities of surfactants, as depicted in the Table 1, were dissolved in water to prepare the stabilizer solutions. The TDF suspended (coarse particle) stabilizer solutions consist of 10 and 20% (w/w) were homogenized with an Ultra-Turrax® T25 (IKA, Sweden) equipped with a dispensing tool (S25 N-10G) for 10 and 30 min, respectively at 16,000 rpm. The rate of shear and time were selected and optimized based on previous experience (Kushwaha et al., 2013; Singh et al., 2014). The temperature was maintained at 6–10 °C using ice-bath to prevent thermally induced particle aggregation or degradation.

3.2. Preparation of casting film gel

The casting film (placebo) gel consists of HPMC (20%), glycerol - propylene glycol (3%), and sweetener - flavors (2–4%) in w/w ratios relative to the total weight of the gel. Initially, excipients were dissolved in water and then HPMC was gradually added to this solution under constant magnetic stirring (800 rpm) at ambient temperature (21 ± 1 °C). The resulting solution was allowed to stir for 3–4 h until the formation of homogenous casting film gel. To this casting film gel, TDF nanosuspensions were added (1 part of nanosuspension and 2 parts of placebo film casting gel) and stirred constantly using magnetic stirrer (500 rpm) at ambient temperature. This gel was kept aside for 3–4 h to remove the air bubbles.

Table 1
Concentration of the surfactants and drug loads (as nanocrystals) used in the films.

Formulation (F)	HPMC (% w/w)	F-68 (% w/w)	Vitamin E TPGS (% w/w)	Tadalafil (% w/w)
1	2.5	–	–	10
2	2.5	0.03	–	10
3	2.5	0.5	–	10
4	2.5	–	0.02	10
5	2.5	–	0.5	10
6	2.5	–	–	20
7	2.5	0.03	–	20
8	2.5	0.5	–	20
9	2.5	–	0.02	20
10	2.5	–	0.5	20
Placebo	2.5	–	–	–

3.3. Preparation of placebo and nanocrystal drug loaded films

A 9 g of placebo or nanocrystal mixed gel were casted on a fluoropolymer coated polyester sheet (Scotchpak® release liner 1022, 3 M Inc., USA) using an automated film applicator equipped with a coating knife (Coatmaster 510, Erichsen, Sweden). A fixed wet film thickness (550 μm) and casting speed (5 mm/s) were used. The wet film thickness was calculated based on formula as mentioned elsewhere (Preis et al., 2012). The drug loads in 6 cm^2 film were 10 mg (F1–F5) and 20 mg (F6–F10). The casted films were dried using convective hot air oven (Binder, Sweden) at 60 °C for 45 min. TDF thermal stability at drying temperature was observed in preliminary tests by TGA and HPLC methods (data not shown). After drying, films were carefully peeled and sealed in plastic zip (polythene) pouches. The samples were stored in a desiccator (23 °C/40% RH) until further characterization.

3.4. Particle size, polydispersity index and zeta potential

The particle size (PS), polydispersity index (PDI) and zeta potential (ZP) were determined using a Zetasizer (Malvern, UK) at 25 °C. One milliliter of nanocrystal suspension was withdrawn after 2 h of the preparation and a 1 × 1 cm^2 TDF nanocrystal-loaded film were redispersed at 1:10 ratio (v/v), respectively in corresponding stabilizer solution and vortexed for 1 min. PS, PDI, ZP were measured using three different samples of each batch.

3.5. Dry film thickness

The thickness of the films was measured using a vernier caliper (Cokraft®, Digital caliper, Sweden). Thickness was measured at three different locations across the film and then the average and standard deviation was calculated.

3.6. Differential scanning calorimetry (DSC)

Thermograms of samples (pure TDF and films) were recorded using differential scanning calorimeter (TA Instruments Q 1000, USA) equipped with refrigerated cooling system. Each sample (2–5 mg) was placed in an aluminum pan and non-hermetically sealed. The samples were heated at a rate of 10 °C/min in the range 25–300 °C under nitrogen purge (50 mL/min). The DSC was previously calibrated for temperature and heat capacities using indium and sapphire. Results were analyzed using Universal analysis software (TA instruments, USA).

3.7. Thermo-gravimetric analysis (TGA)

Thermo-gravimetric analysis was performed using a TGA instrument (TA instruments, USA) to determine the moisture content in the film. Approximately 5–8 mg of the film (small pieces) was placed in platinum pan and heated from 25 to 150 °C at a constant heating rate (10 °C/min) under nitrogen flow (50 mL/min). Results were analyzed using Universal analysis software (TA instruments, USA).

3.8. Powder X-ray diffraction (PXRD)

PXRD patterns of film samples were collected by X-ray Diffractometer (X'Pert PRO, PANalytical, Netherlands) equipped with a PIXel3D detector and a monochromatic Cu Kα radiation X-Ray tube radiation (λ = 1.54056 Å). The samples (3 × 3 cm^2 films) were placed on a silicone (zero back ground) plate which was fitted in the sample metal holder. Samples were scanned in the 2θ (diffraction angle) between 5° and 40° increasing at a step size of 0.02. Voltage and current of 45 kV and 40 mA radiation was used, respectively. All patterns were obtained at 25 ± 1 °C. The data were processed using HighScore Plus software (PANalytical, The Netherlands).

3.9. Mechanical properties

Mechanical properties were measured using TA.XTPlus texture analyzer (Stable Micro Systems, UK) equipped with a 5 kg load cell as previously described (Morales et al., 2013; Morales et al., 2014). Films were cut in rectangular strips of 1 × 5 cm^2 and 1 × 1 cm^2 on each end were held between clamps attached to the texture analyzer. Thus, the effective testing area was 1 × 3 cm^2. The upper clamp (connected to the mobile arm of the texture analyzer) stretches the film upwards at a rate of 0.5 mm/s until film fracture. Stress was determined from the force measurements obtained from the instrument divided by the cross-sectional area of the film, while strain was calculated by dividing the increase in length by the initial film length. From the stress vs strain plot, the tensile strength and the elongation at break were obtained from the peak stress and the maximum strain, respectively, also represented by the following equations:

$$\text{Tensile strength (TS)} = \frac{\text{Peak stress}}{\text{Cross} - \text{sectional area of film}} \quad (1)$$

$$\text{Elongation at break (EB)} = \frac{\text{Increase in length at break}}{\text{Initial film length}} \times 100 \quad (2)$$

In addition, the Young's modulus (elastic modulus) was obtained from the initial elastic deformation area in the stress vs strain plot. Since the rate of the mobile arm extension was constant for all films tested, direct comparison of the slope in this region can be done.

3.10. Scanning electron microscopy (SEM)

Surface and cross-section morphology of films was observed by scanning electron microscopy (SEM) in an Inspect F50 (FEI, Hillsboro, OR, USA). Film cross-sections were obtained by immersion in liquid nitrogen, fixed on aluminum stubs by conductive carbon tape, and sputter-coated with gold (approx. 10–12 nm) in a high vacuum evaporator (108 Auto, Cressington Scientific Instruments Ltd., UK).

3.11. Atomic force microscope (AFM)

The surface morphology of selected films was visualized using an atomic force microscope (AFM) Nanoscope V from Veeco, USA, at a resonance frequency of 70 kHz and a spring constant of 1–5 N/m. Film samples were mounted on mica substrates prior to capturing images. The film surface characteristics and roughness were studied using the Nanoscope V software.

3.12. HPLC analytical method

A high performance liquid chromatograph system (Agilent systems Inc., USA) with an auto sampler was used for the analysis. The sample separation was performed on an Agilent Hypersil C18 column (5 μm, 150 mm × 4.6 mm) with the mobile phase consisting of acetonitrile and 10 mM phosphate buffer (pH 7.0) with a ratio of 60:40 (v/v) at ambient temperature. The flow rate was kept at 0.8 mL/min and the determination wavelength was 262 nm. The calibration curve was prepared in range of 1–500 μg/mL in solvent [60:40 (v/v) of acetonitrile and water]. The data was recorded using millennium solutions software (Reddy et al., 2010). The method was validated as per ICH Q2 and USP guidelines for the parameters like system suitability, selectivity, linearity, accuracy, precision, and robustness.

3.13. Drug content

Films (1 × 1 cm^2) were placed in a volumetric flask containing 50 mL of water and acetonitrile [1:1, (v/v)] mixture and kept under magnetic stirring at 100 rpm for 1 h. The obtained solution was filtered through the syringe filter (0.45 μm) and 1 mL of the filtrate was

analyzed for drug content by HPLC method described in section 3.12. (Reddy et al., 2010).

3.14. Disintegration time

Disintegration time of the films was evaluated by modified Petri dish method (Garsuch and Breitkreutz, 2010). Samples (1 × 1 cm^2) were placed in a Petri dish containing 2 mL of water, and were shaken at 60 rpm using arbitral shaker water bath at 37 ± 1 °C. The time until film disintegration or disruption was recorded with a stopwatch.

3.15. Solubility studies

The solubility of TDF was determined in water, 0.5% SLS, 2.5% of HPMC + 0.5% of pluronic F-68 and 2.5% of HPMC + 0.5% of Vitamin E TPGS. Briefly, the excessive amount (300 mg) of TDF was added in six conical flasks each containing 20 mL of water and other respective polymer-surfactant solutions. The flasks were tightly corked, placed in a thermostat coupled water bath at 25 °C (37 °C in case of SLS) and agitated at 70 rpm for 48 h. After this period, separated aliquots from each flask were filtered through 0.45 µm filter then diluted with solutions and analyzed using HPLC. Each solubility value was determined in triplicate (n = 3) and the results were reported as mean ± standard deviation (SD).

3.16. In vitro dissolution

In vitro dissolution studies of films were carried out using dissolution apparatus (USP-II) at 37 ± 0.5 °C. A 500 mL of 0.5% (w/v) sodium lauryl sulfate solution was used as a dissolution medium and stirred at 50 rpm (Vyas et al., 2009). Films (F1–F10) of 2 × 3 cm sizes (10 and 20 mg) were carefully dropped into dissolution medium. The samples (5 mL) were withdrawn at different time intervals and simultaneously replaced with similar amount of fresh dissolution media. The samples were filtered using syringe filters (0.45 µm) and the filtrate was analyzed by HPLC method as described in section 3.12.

3.17. Statistical analysis

The Student t-test for two group comparisons and one-way ANOVA with Tukey's post hoc multiple comparisons were used to determine statistically significant differences ($p < 0.05$). All results were expressed as average and standard deviation of triplicates whereas mechanical properties were presented with n = 5.

4. Results and discussion

4.1. Nanosuspensions and their incorporation into films

4.1.1. Properties of freshly prepared nanosupensions

Tadalafil nanosuspensions were prepared by high shear homogenization, which is an industrially relevant and widely used technique. The size (d_{90}) and PDI of nanocrystals (freshly prepared) and redispersed nanocrystals (post-loading into films) are shown in Fig. 1a and b, respectively.

As can be seen in the Fig. 1a, the particle size was 588–945 nm in freshly prepared nanosuspensions. In the case of 10% drug load, particle size of F1 (HPMC alone) was significantly ($p < 0.05$) lower than F2-F5 which contain stabilizers, HPMC and surfactants (pluronic F-68 or TPGS) at different concentrations [0.02–0.5% (w/w)]. In contrast, there was no significant difference observed among F6-F10 (except F8) containing higher drug load i.e. 20% (w/w). When HMPC was used alone, a significant ($P < 0.05$) increase in particle size was observed with increasing drug load from 10 to 20% (w/w) (F1 vs F6). No significant difference in particle size was observed when concentrations of stabilizers (pluronic F-68 and TPGS) increased from 0.02 to 0.5% (w/w)

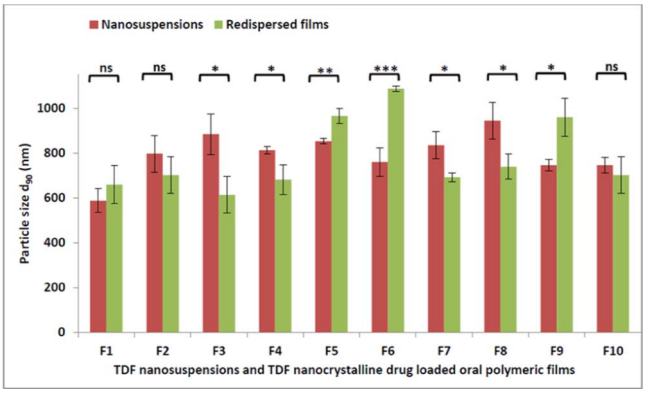

1(a)

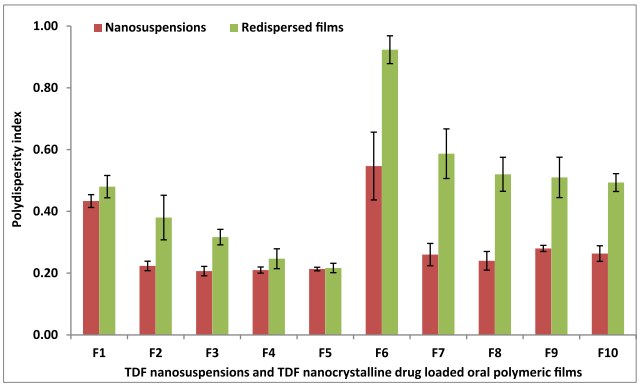

1(b)

Fig. 1. (a) Particle size (d_{90}) of nanosuspensions and from redispersed films. (b) Polydispersity indexes of nanosuspensions and from redispersed films. Particle size between nanosuspension and redispersed films are mentioned where statistical difference is $p < 0.05$ Each value denotes Mean ± SD (n = 3).

at different drug loads.

Surfactants (pluronic F-68 and TPGS) are non-ionic but have varied physicochemical properties and their use as stabilizers in various pharmaceutical preparations has been well documented (Loh et al., 2015). Both of the surfactants have been widely used in different nanocolloidal drug delivery systems. However, the role of pluronic F-68/TPGS in combination with HPMC for the stabilization of nanosuspensions in pertinent to orodispersible films perspective has not been studied. Thus, it could be interesting to understand the effect of polymer-surfactant combination on the stabilization of nanosuspensions and their effect on physico mechanical and dissolution properties. The solubility of TDF in pluronic F-68 and TPGS [0.5% (w/w)] in the presence of HPMC [2.5% (w/w)] was found to be 3.12 ± 0.23 µg/mL and 3.09 ± 0.63 µg/mL, respectively, which is not very different from its solubility in water (2.86 µg/mL); hence, surfactant concentrations in the range [0.02–0.5% (w/w)] were selected in the study. The above particle size result suggests that HPMC alone or in combination with pluronic F-68 or TPGS is suitable to produce and stabilize nanocrystals in the range 588–945 nm. However, the slight increase in particle size after addition of pluronic F-68/TPGS (both concentrations) at both drug loads could be attributed to poor adsorption of stabilizers on the surface of newly generated nanocrystals, due to inter-intra molecular interactions between HPMC and surfactants under shear energy. Obeidat et al. has also observed similar trends with TDF nanosuspensions in the presence of HPMC and pluronic F-127. The polydispersity indexes of different batches can be seen in Fig. 1b that indicate the narrow dispersity of nanosuspensions except prepared without additional surfactants (F1 & F6). The weak negative to near neutral zeta potential of nanosuspensions (− 1.79 to − 6.34 mV) could be explained by the nonionic nature and suggests possible steric stabilization mechanism of

surfactants (Tuomela et al., 2016). Further, nanocrystals were stable in tested period (2, 6 and 24 h) in terms of particle size and PDI.

4.1.2. Nanocrystal properties from redispersed films

Redispersiblity of nanocrystals from the film when in contact with aqueous media is essential for rapid dissolution of the drug. The particle size of redispersed TDF nanocystals is shown in Fig. 1a. The particle size (d_{90}) range of redispersed nanocrystals from different films was 614–1087 nm. In the case of 10% drug load, particle size of F1–F4 was significantly ($p < 0.05$) lower than F5 whereas no trends were observed at 20% drug load. In general, the differences in the particle size between HPMC alone and HPMC/surfactants were evident at 20% drug load. Further, it was noticed that redispersed films containing pluronic F-68 and TPGS surfactants particle size was slightly less (except F5 and F9) when compared to respective nanosuspensions. On the other hand, higher particle size was observed in the case of redispersed film (F6) containing HPMC alone. This suggests that adequate use of surfactants not only helps stabilize nanocrystals but also facilitates uniform dispersion into casting gel during mixing, and later enables acceptable recovery of the nanocrystals during redispersion. These results are in good agreement with the work where redispersed films particles size was shown to be less compared to their precursor nanosuspensions (Krull et al., 2016). Bhakay et al. reported that the presence of higher concentrations of HPMC (in film casting gel) allows better distribution of particles in films due to effective encapsulation of the hydrophobic drug nanocystals in a hydrophilic film matrix (Bhakay et al., 2016). The noticeable changes in PDI of particles from redispersed films were also observed and the differences were highly evident in formulations F6–F10 (fig. 1b). It may be due to the physical surface adsorption of HPMC monomers (polymer available in films) on the TDF nanocrystals that eventually form reversible nanoclusters. Krull et al. observed changes in particle properties because of formation of drug-polymer agglomerates or clusters during redispersion test (Krull et al., 2017). However, this study suggests that combination of HPMC and surfactants is beneficial for nanocrystal distribution, stabilization and redispersion from films.

4.2. Solid state of the film

Pure TDF and nanocrystalline TDF loaded films were assessed for their thermal properties. The representative thermograms are shown in Fig. 2. The pure TDF has shown single sharp endothermic peak T_{onset} at 304.95 °C suggesting that the raw material was crystalline. It corroborates with the earlier reported melting points of crystalline TDF (Mehanna et al., 2010; Park et al., 2014; Wlodarski et al., 2015). As can be seen in the Fig. 2, endothermic peaks corresponding to the melting of TDF were observed at 270–282 °C (T_{onset}) in the representative films; F1, F3 and F10. The depression in the melting point and heat of fusion could be attributed to the presence of larger concentration of HPMC.

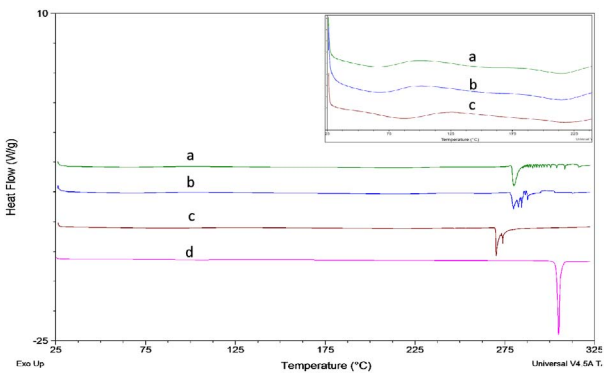

Fig. 2. DSC thermograms: a. TDF nanocrystals loaded films-F1, b. F3, c. F10 and d. Pure TDF.

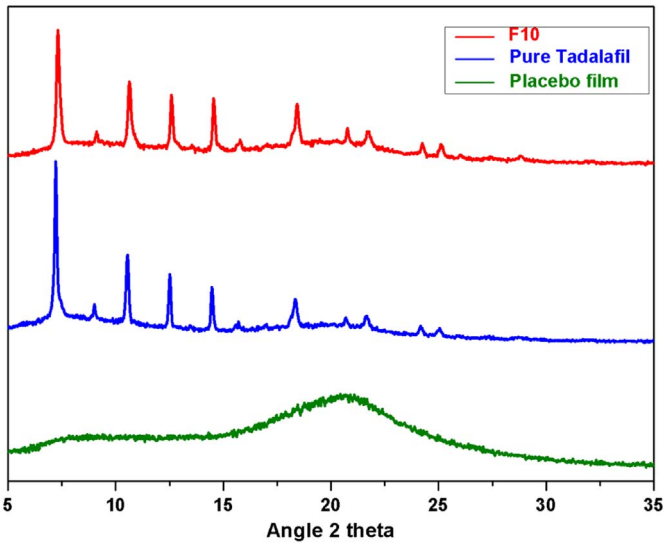

Fig. 3. PXRD patterns of Placebo film, pure TDF and TDF nanocrystals loaded film (F10).

Additionally, a broad endothermic peak corresponding to the melting of pluronic F-68/TPGS at 25–60 °C and the T_g of HMPC at approx. 140 °C were observed (insert in Fig. 2). It suggests that TDF is incorporated in the nanocrystalline form in polymer matrix. Mehanna et al., were unable to detect the melting point in physical mixture of TDF and pluronic F-127 at 1:5 ratios (w/w) which is attributed to dissolution or melting of drug in higher amount of surfactant during the DSC process (Mehanna et al., 2010).

Powder X-ray diffraction was used for further evaluation of crystalline nature of TDF in polymeric films. The PXRD patterns of pure TDF and representative films are shown in Fig. 3. The PXRD pattern of pure TDF revealed its crystalline state and the representative film (F10) exhibited crystalline state that was identical to pure form PXRD patterns. The PXRD results corroborated the results of DSC and confirmed the crystalline state of TDF in films.

4.3. Mechanical properties

Young's modulus (elastic modulus), tensile strength and elongation at break of films are shown in Fig. 4(a–c). Mechanical properties of nanocrystal TDF-loaded films were significantly different compared to placebo film ($P < 0.05$). Young's modulus changes are insignificant among films (10 mg) F1 vs F2–F5 (except F2) (Fig. 4a). However, young's modulus was reduced significantly when increasing pluronic F-68 from 0.03% (w/w) (F2) to 0.5% (w/w) (F3) but it was not observed with TPGS (F4 vs F5). It indicates pluronic F-68 at 0.5% (w/w) may be acting as a plasticizer leading to higher deformation. On other hand, significant decrease in young's modulus was observed upon addition of surfactants when comparing of results of films (20 mg) F6 Vs F7–F10 (except F10). The young's modulus results suggest that an increased drug load (nanocrystals) or surfactants could significantly changes the stiffness of the films.

In case of tensile strength, it was observed that addition of surfactants may significantly increase tensile strength when comparing films (10 mg); F1 vs F2–F5 (Fig. 4b) but not observed in case of films (20 mg); F6 vs F10. It was also noticed in films (10 mg) that increasing of pluronic F-68 from 0.03% (w/w) (F2) to 0.5% (w/w) (F3) reduces tensile strength in contrast to films (20 mg) F7 vs F8. There was no significant change observed while increasing of TPGS at both drug loads.

In case of elongation at break, films F1 vs F6 (vary in drug load but no additional surfactant) show insignificant differences (Fig. 4c). Films (10 mg) F1 vs F2–F5 show significant differences in their elongation

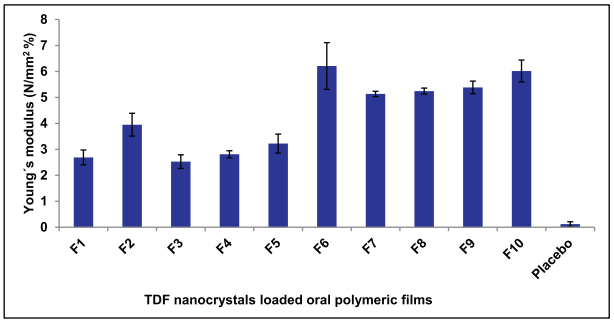

(a) Young´s modulus

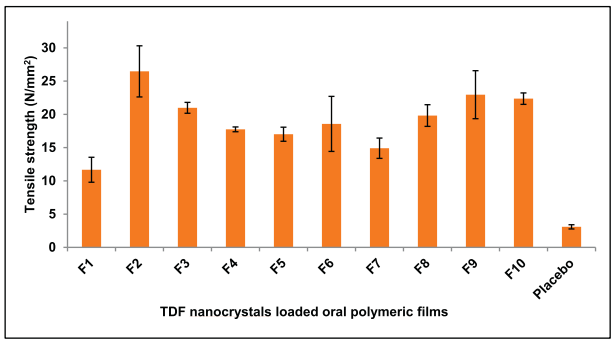

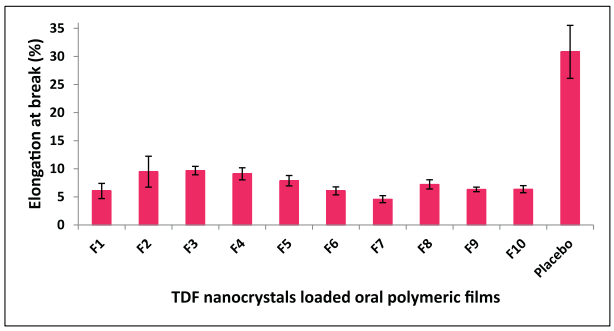

(c) Elongation at break

Fig. 4. Mechanical properties of different TDF nanocrystals loaded films (a) Young's modulus (b) tensile strength (c) elongation at break.
Each value denotes Mean ± SD (n = 5).

except F5 but it is insignificant in films (20 mg) F6 vs F7–F10.

Mechanical properties are important quality attributes of films. In fact, the mechanical properties alone shall decide the quality and elegance of the film. However, there are no official standards described elsewhere about mechanical properties of oral films. Polymer type, plasticizers, moisture content, drying rate, amount of solids and particle size are governing factors for corresponding mechanical properties of materials (Karki et al., 2016). Preis et al., thoroughly investigated mechanical properties of commercial and in-house manufactured oral films by a modified methodology and proposed appropriate range of mechanical properties that could be considered as reference (Preis et al., 2014). Visser et al., studied effect of polymer, plasticizer and drying rate by DoE to understand their role on mechanical properties as critical quality attributes (Visser et al., 2015a). The above studies suggest certain range of mechanical properties which are important for manufacturing, packing and stability. Despite this guidance, mechanical properties that have adequate flexibility and non-interference in disintegration of films are recommendable.

Initially, moisture/water content was analyzed by TGA. The observed weight loss was between 1.2 and 1.6% in films (F1 to F10). The representative thermograms (F1 and F6) are shown in supplementary data (Fig. S-1). The bulky nature of the HPMC and inherent water might be a possible reason for presence of some moisture content in the films. Further, TGA data suggested that films retained a small amount of water and conditions of drying time and temperature (60 °C at 45 min) were adequate. Films were prepared with constant polymer-plasticizer ratios in this study, including process parameters i.e. fixed wet film thickness and casting rate. Therefore, we can assume that the observed mechanical properties have direct influence on drug load, type and amount of surfactants. The above results revealed the influence of surfactant and drug load on films mechanical properties. Interestingly, surfactants and their concentrations used in this study could not produce very drastic changes but certainly showed distinctive differences in their mechanical properties. It may be possible due to plasticization behavior of surfactants F-68 and TPGS. The mechanical properties are more distinctive in films of 10 mg (lower) drug load than 20 mg (higher). Varying surfactant to solid contents (drug nanocrystals and film excipients) ratio may be an appropriate reason behind this observation. Films (F1 to F10) are viable in handling during peeling, cutting and packaging at laboratory level despite of their differences in mechanical properties. It is interesting to mention that the observed young's modulus, tensile strength and elongation at break results correlated well with the literature reports of HPMC based films (Visser et al., 2015a).

4.4. Film morphology

Film morphology of TDF nanocrystals loaded films was observed by the SEM. The SEM micrographs of films cross-sections (F1–F10) are shown in Fig. 5. It can be seen that F1–F5 had lower concentration of nanocrystals compared to F6-F10, due to differences in their drug load. The SEM micrograph of films (F1–F10) qualitatively illustrates homogenous dispersion of TDF nanocrystals in HPMC polymer matrix. No large micro agglomerates were observed but prominent nanocrystal clusters can be seen in the films (Fig. 5; F6–F10). The SEM micrograph cross-section of placebo film showed homogenous micro structure with slight fractures. Krull et al., reported similar SEM micrographs related surfactant free polymer strip films containing poorly soluble drugs in nanonized state (Krull et al., 2015).

AFM study was also performed to get better understanding of the existence of nanocrystals in polymer matrix as a complementary tool to SEM to investigate film surface. Quantitative film surface roughness was also studied by AFM. The AFM images of representative film (F10) with drug load (20 mg) is shown in Fig. 6a and b. AFM images showed TDF nanocrystals in polymer matrix with small clusters at submicron scale (circled in blue color). The surface roughness is one of the useful parameters that describes qualitative and quantitative information about the appearance and existence of the particles, while mixing of two distinctive materials. AFM can also be used to get insights on the crystalline behavior of the material. The surface roughness values (Rq) for 10 mg and 20 mg films were 43 and 108 nm, respectively suggesting that higher the drug load greater will be surface roughness. It further confirmed the TDF nanocrystals existence in films which corresponds to drug load. Thus, the SEM and AFM results are correlated with each other.

4.5. Thickness and drug content

The thickness and drug content results are shown in Table 2. The thickness of the films ranged between 81 and 96 μm. The films (F2) and (F1) had highest (96 ± 11) and lowest (81 ± 1) thickness, respectively. The drug content for films is shown in Table 2. The drug content ranged between 94 and 102%. It indicated that TDF nanocrystals were uniformly mixed with HPMC polymer casting film gel. The formulation (F7) and (F9) had the highest (102 ± 5) and lowest (94 ± 4) drug content, respectively. In general, the drug content was in acceptable limits according to USP. The slight difference in thickness of films might be due to variation in the density/solid content of casting film gel of

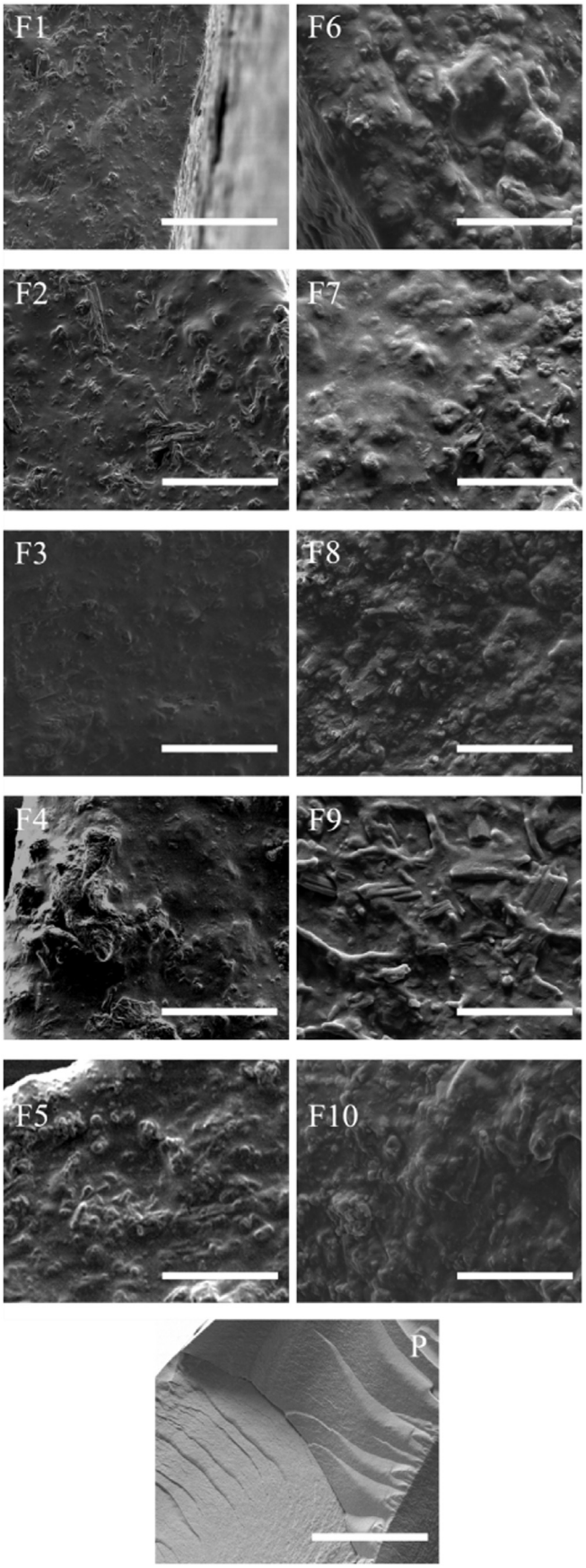

Fig. 5. Cross-sectional SEM micrographs of TDF nanocrystals loaded films (F1–F10) and placebo film (P). The bar represents 30 μm.

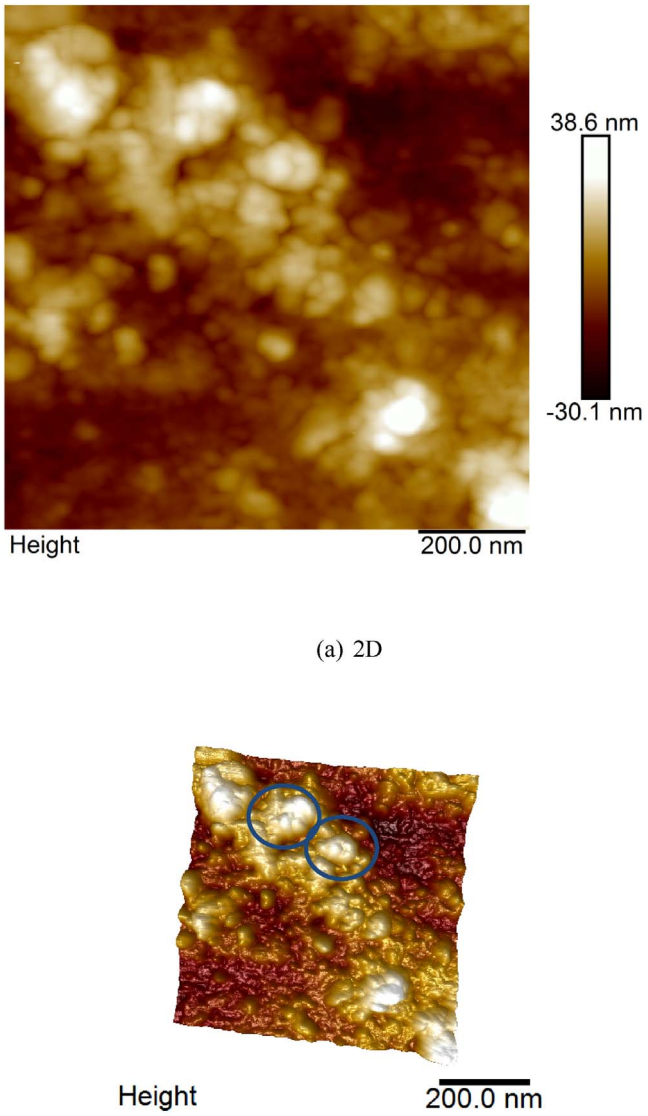

Fig. 6. AFM surface images of (a) 2D image of TDF nanocrystal loaded film (F10) (b) 3D image of TDF nanocrystal loaded film (F10). (For interpretation of the references to color in this figure, the reader is referred to the web version of this article.)

Table 2
Thickness, drug content uniformity and disintegration times of different films (1 × 1 cm) Each value denotes Mean ± SD (n = 3).

Formulation (F)	Thickness (μm)	Drug content (mg)	Disintegration time (min)
1	81 ± 01	96.90 ± 1.21	7.02 ± 0.02
2	96 ± 11	101.20 ± 1.10	4.04 ± 0.03
3	93 ± 05	98.90 ± 4.50	4.13 ± 0.01
4	83 ± 05	100.00 ± 7.60	4.05 ± 0.05
5	83 ± 05	100.00 ± 3.20	8.13 ± 0.05
6	93 ± 05	99.15 ± 1.11	7.22 ± 0.01
7	95 ± 15	102.05 ± 5.55	15.40 ± 0.01
8	83 ± 05	100.11 ± 4.94	4.04 ± 0.02
9	81 ± 02	95.55 ± 4.65	11.18 ± 0.02
10	87 ± 06	94.05 ± 4.21	14.57 ± 0.27

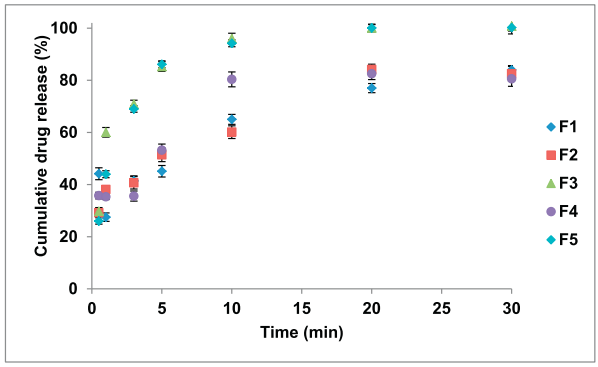

(a)

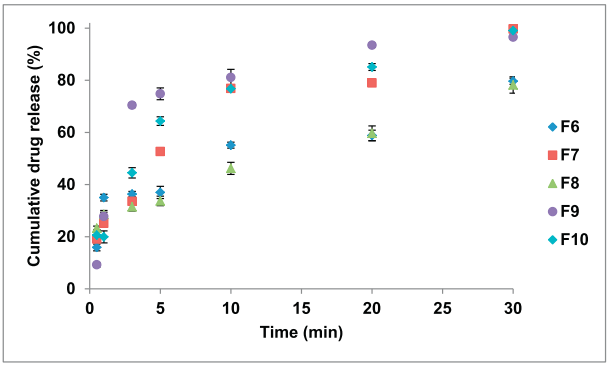

(b)

Fig. 7. Dissolution profiles of (a) TDF nanocrystals-loaded film of 10 mg/6 cm^2 (F1–F5) and (b) TDF nanocrystals-loaded film of 20 mg/6 cm^2 (F6–F10).
Each value denotes Mean ± SD (n = 3).

respective formulations. However, process parameters were not responsible, since they were constant during film casting and also films treated similarly until their storage.

4.6. Disintegration time

Modified Petri dish method was used for assessing of disintegration time in this study. The disintegration time results are shown in Table 2. As can be seen from the results, films containing HPMC/surfactant disintegrated faster than HPMC alone. Surfactant pluronic F-68 favored disintegration of films as compared to TPGS at different drug loads. The disintegration time of approximately 4 min was observed in films with pluronic F-68 at 0.5% (w/w). Disintegration is considered as one of the important characteristics for the performance of oral films. However, there is no official method to determine disintegration of oral films. Different formulation aspects like type and amount of polymer, solids content, drug solubility, surfactants and plasticizers are required to optimize to get desired disintegration time. In general, disintegration/dissolution is dependent on surface tension, wettability, porosity, disintegration media, and intra- and inter-molecular interactions between composed polymer materials (Miller-Chou and Koenig, 2003). Thus, pluronic F-68 or TPGS based films might have reduced surface tension and thereby enhanced wettability leading to better disintegration.

4.7. Dissolution

The dissolutions studies were carried out under non-sink condition. Liu et al. reported that carrying of non-sink dissolution would be suitable for proper discrimination of dissolution profiles of nanosuspensions (Liu et al., 2013). In fact, Krull et al. employed non-sink dissolution experiments for studying drug release profiles of nanoparticles loaded polymer films (Krull et al., 2016). Therefore, we have also performed dissolution studies under non-sink condition (solubility of pure TDF in dissolution medium was 79.9 ± 1.2 µg/mL). Dissolution results of films are shown in Fig. 7a and b. The $t_{80\%}$ of TDF release was observed between 3 and 30 min in films (both drug loads). Films with TPGS [0.02 and 0.5% (w/w)] had faster dissolution rate (both drug loads) than other films. The $t_{80\%}$ of TDF release was 3 and 10 min for films (containing 0.5% of TPGS) F5 and F10, respectively. Films with pluronic F-68 [0.02 and 0.5% (w/w)] increased the dissolution rate only in case of 10 mg drug load. It can also be seen that 10 mg drug load film had faster dissolution rate as compare to those with 20 mg drug load films. The results illustrated that increasing drug load prolonged the dissolution rate. Further, the significant differences in young's modulus (at both drug loads) explain film rigidity that could also influence the film wettability, water penetration into polymer network followed by changes in dissolution rate. Based on the redispersed particle size results, it was important to mention that the particle size of TDF nanocrystals might not have influenced the dissolution rate as all films contain relatively similar particle size (average is 700 nm) except F6 and F9. Thus, it is reasonable to suggest the differences in dissolution rate depend mainly on the concentration of the surfactant in the respective film. It was noticed that films with TPGS showed better dissolution relative to higher drug loads. The quicker formation of TPGS micelles in the presence of SLS (component of dissolution media) than pluronic F-68 could be the probable reason for this dissolution enhancement. Several reports stated that TPGS is a potential solubility and absorption enhancer that is widely used for bioavailability enhancement of oral formulations (Guo et al., 2013). The present study also demonstrated the ability of surfactant (TPGS) to enhance the dissolution rate of nanocrystalline TDF (poorly soluble) loaded in polymeric films intended for GIT absorption. Thus, the addition of surfactants was necessary in oral films for improvement of dissolution and maintaining of stability of TDF nanocrystals.

5. Conclusion

TDF nanocrystal loaded OFs were prepared successfully by high shear homogenization based nanonization followed by solvent casting. Addition of pluronic F-68/TPGS was shown to be preferable in the preparation of TDF nanosuspensions. TDF nanocrystals were confirmed to be homogenously dispersed in the polymeric matrix of casting gel and were found to retain nanosize in the films. The present study confirmed that mechanical, disintegration and dissolution properties were dependent on the concentration of surfactants and drug loads. It was found that the addition of surfactant; TPGS at 0.02–0.5% (w/w) was necessary for dissolution enhancement of TDF films. Finally, it can be concluded that the addition of surfactants (type and amount) was important in the development of OFs with poorly water soluble drugs to get desired dissolution properties. However, the benefits may depend on surfactant inter- and intra- molecular interactions with drug and polymer that would apparently changes the wettability and solubility with respective to media or at the site of dissolution/absorption. Furthermore, employed strategies i.e. converting of nanosuspensions (liquid form) into nanocrystal (solid form) could be utilized in the development of nanosized solid dosage forms of poorly soluble drugs.

Supplementary data to this article can be found online at http://dx.doi.org/10.1016/j.ejps.2017.08.019.

Acknowledgements

PRV and SV are gratefully for the financial assistance of Kempe Foundation, Sweden. PRV also acknowledges the financial assistance of The Swedish Pharmaceutical Society, Sweden. JOM acknowledges the financial support from FONDAP 15130011 and FONDECYT 11130235.

References

Badr-Eldin, S.M., Elkheshen, S.A., Ghorab, M.M., 2008. Inclusion complexes of tadalafil with natural and chemically modified β-cyclodextrins. I: Preparation and in-vitro evaluation. Eur. J. Pharm. Biopharm. 70, 819–827.

Beck, C., Sievens-Figueroa, L., Gärtner, K., Jerez-Rozo, J.I., Romañach, R.J., Bilgili, E., Davé, R.N., 2013. Effects of stabilizers on particle redispersion and dissolution from polymer strip films containing liquid antisolvent precipitated griseofulvin particles. Powder Technol. 37–51.

Bhakay, A., Vizzotti, E., Li, M., Davé, R., Bilgili, E., 2016. Incorporation of fenofibrate nanoparticles prepared by melt emulsification into polymeric films. J. Pharm. Innov. 11, 53–63.

Bhosle, M., Benner, J.S., DeKoven, M., Shelton, J., 2009. Difficult to Swallow: Patient Preferences for Alternative Valproate Pharmaceutical Formulations. Patient Preference and Adherence. 3. pp. 161–171.

Buanz, A.B., Saunders, M.H., Basit, A.W., Gaisford, S., 2011. Preparation of personalized-dose salbutamol sulphate oral films with thermal ink-jet printing. Pharm. Res. 28, 2386–2392.

Buanz, A.B., Belaunde, C.C., Soutari, N., Tuleu, C., Gul, M.O., Gaisford, S., 2015. Ink-jet printing versus solvent casting to prepare oral films: effect on mechanical properties and physical stability. Int. J. Pharm. 494, 611–618.

Choi, J., Park, J., 2017. Design of PVP/VA S-630 based tadalafil solid dispersion to enhance the dissolution rate. Eur. J. Pharm. Sci. 97, 269–276.

Dixit, R.P., Puthli, S.P., 2009. Oral strip technology: overview and future potential. J. J. Control. Release 139, 94–107.

Frajese, G.V., Pozzi, F., Frajese, G., 2006. Tadalafil in the treatment of erectile dysfunction; an overview of the clinical evidence. Clin. Interv. Aging 1, 439–449.

Garsuch, V., Breitkreutz, J., 2010. Comparative investigations on different polymers for the preparation of fast-dissolving oral films. J. Pharm. Pharmacol. 62, 539–545.

Guo, Y., Luo, J., Tan, S., Otieno, B.O., Zhang, Z., 2013. The applications of vitamin E TPGS in drug delivery. Eur. J. Pharm. Sci. 49, 175–186.

Hoffmann, E.M., Breitenbach, A., Breitkreutz, J., 2011. Advances in orodispersible films for drug delivery. Expert Opin. Drug Deliv. 8, 299–316.

Illangakoon, U.E., Gill, H., Shearman, G.C., Parhizkar, M., Mahalingam, S., Chatterton, N.P., Williams, G.R., 2014. Fast dissolving paracetamol/caffeine nanofibers prepared by electrospinning. Int. J. Pharm. 477, 369–379.

Junghanns, J.A.H., Muller, R.H., 2008. Nanocrystal technology, drug delivery and clinical applications. Int. J. Nanomedicine 3, 295–310.

Karki, S., Kim, H., Na, S., Shin, D., Jo, K., Lee, J., 2016. Thin films as an emerging platform for drug delivery. Asian J. Pharm. Sci. 11 (5), 559–574.

Kathpalia, H., Gupte, A., 2013. An introduction to fast dissolving oral thin film drug delivery systems: a review. Curr. Drug Deliv. 10, 667–684.

Krull, S.M., Susarla, R., Afolabi, A., Li, M., Ying, Y., Iqbal, Z., Bilgili, E., Davé, R.N., 2015. Polymer strip films as a robust, surfactant-free platform for delivery of BCS class II drug nanoparticles. Int. J. Pharm. 489, 45–57.

Krull, S.M., Ma, Z., Li, M., Davé, R.N., Bilgili, E., 2016. Preparation and characterization of fast dissolving pullulan films containing BCS class II drug nanoparticles for bioavailability enhancement. Drug Dev. Ind. Pharm. 42, 1073–1085.

Krull, S.M., Moreno, J., Li, M., Bilgili, E., Davé, R.N., 2017. Critical material attributes (CMAs) of strip films loaded with poorly water-soluble drug nanoparticles: III. Impact of drug nanoparticle loading. Int. J. Pharm. 523, 33–41.

Kushwaha, A.K., Vuddanda, P.R., Karunanidhi, P., Singh, S.K., Singh, S., 2013. Development and evaluation of solid lipid nanoparticles of raloxifene hydrochloride for enhanced bioavailability. Biomed. Res. Int. 2013, 584549.

Liu, P., De Wulf, O., Laru, J., Heikkilä, T., van Veen, B., Kiesvaara, J., Hirvonen, J., Peltonen, L., Laaksonen, T., 2013. Dissolution studies of poorly soluble drug nanosuspensions in non-sink conditions. AAPS PharmSciTech 14, 748–756.

Loh, Z.H., Samanta, A.K., Sia Heng, P.W., 2015. Overview of milling techniques for improving the solubility of poorly water-soluble drugs. Asian J. Pharm. Sci. 10, 255–274.

Mehanna, M.M., Motawaa, A.M., Samaha, M.W., 2010. In sight into tadalafil–block copolymer binary solid dispersion: mechanistic investigation of dissolution enhancement. Int. J. Pharm. 402, 78–88.

Miller-Chou, B., Koenig, J., 2003. A review of polymer dissolution. Prog. Polym. Sci. 28, 1223–1270.

Morales, J.O., Ross, A.C., McConville, J.T., 2013. Protein-coated nanoparticles embedded in films as delivery platforms. J. Pharm. Pharmacol. 65, 827–838.

Morales, J.O., Huang, S., Williams III, R.O., McConville, J.T., 2014. Films loaded with insulin-coated nanoparticles (ICNP) as potential platforms for peptide buccal delivery. Colloids Surf. B: Biointerfaces 122, 38–45.

Möschwitzer, J.P., 2013. Drug nanocrystals in the commercial pharmaceutical development process. Int. J. Pharm. 453, 142–156.

Obeidat, W.M., Sallam, A.A., 2014. Evaluation of tadalafil nanosuspensions and their PEG solid dispersion matrices for enhancing its dissolution properties. AAPS PharmSciTech 15, 364–374.

Park, J., Cho, W., Kang, H., Lee, B.B.J., Kim, T.S., Hwang, S., 2014. Effect of operating parameters on PVP/tadalafil solid dispersions prepared using supercritical anti-solvent process. J. Supercrit. Fluids 90, 126–133.

Preis, M., Pein, M., Breitkreutz, J., 2012. Development of a taste-masked orodispersible film containing dimenhydrinate. Pharmaceutics 4, 551–562.

Preis, M., Woertz, C., Kleinebudde, P., Breitkreutz, J., 2013. Oromucosal film preparations: classification and characterization methods. Expert Opin. Drug Deliv. 10, 1303–1317.

Preis, M., Knop, K., Breitkreutz, J., 2014. Mechanical strength test for orodispersible and buccal films. Int. J. Pharm. 461, 22–29.

Reddy, B.P., Reddy, K.A., Reddy, M., 2010. Validation and Stability Indicating RP-HPLC Method for the Determination of Tadalafil API in Pharmaceutical Formulations.

Savjani, K.T., Gajjar, A.K., Savjani, J.K., 2012. Drug solubility: importance and enhancement techniques. ISRN Pharmaceutics 2012, 195727.

Sievens-Figueroa, L., Bhakay, A., Jerez-Rozo, J., Pandya, N., Romañach, R.J., Michniak-Kohn, B., Iqbal, Z., Bilgili, E., Davé, R.N., 2012. Preparation and characterization of hydroxypropyl methyl cellulose films containing stable BCS class II drug nanoparticles for pharmaceutical applications. Int. J. Pharm. 423, 496–508.

Singh, B., Vuddanda, P.R.M.R.V., Kumar, V., Saxena, P.S., Singh, S., 2014. Cefuroxime axetil loaded solid lipid nanoparticles for enhanced activity against *S. aureus* biofilm. Colloids Surf. B: Biointerfaces 121, 92–98.

Tang, C., Guan, Y., Yao, S., Zhu, Z., 2014. Preparation of ibuprofen-loaded chitosan films for oral mucosal drug delivery using supercritical solution impregnation. Int. J. Pharm. 473, 434–441.

Tuomela, A., Hirvonen, J., Peltonen, L., 2016. Stabilizing agents for drug nanocrystals: effect on bioavailability. Pharmaceutics 8, 16.

Vinesh, V., Sevukarajan, M., Rajalakshmi, R., Chowdary, G., Haritha, K., 2013. Enhancement of solubility of tadalafil by cocrystal approach. Int. Res. J. Pharm 4, 218–223.

Visser, J.C., Dohmen, W.M., Hinrichs, W.L., Breitkreutz, J., Frijlink, H.W., Woerdenbag, H.J., 2015a. Quality by design approach for optimizing the formulation and physical properties of extemporaneously prepared orodispersible films. Int. J. Pharm. 485, 70–76.

Visser, J.C., Woerdenbag, H.J., Crediet, S., Gerrits, E., Lesschen, M.A., Hinrichs, W.L., Breitkreutz, J., Frijlink, H.W., 2015b. Orodispersible films in individualized pharmacotherapy: the development of a formulation for pharmacy preparations. Int. J. Pharm. 478, 155–163.

Vuddanda, P.R., Mathew, A.P., Velaga, S., 2016. Electrospun nanofiber mats for ultrafast release of ondansetron. React. Funct. Polym. 99, 65–72.

Vyas, V., Sancheti, P., Karekar, P., Shah, M., Pore, Y., 2009. Physicochemical characterization of solid dispersion systems of tadalafil with poloxamer 407. Acta Pharma. 59, 453–461.

Wlodarski, K., Sawicki, W., Haber, K., Knapik, J., Wojnarowska, Z., Paluch, M., Lepek, P., Hawelek, L., Tajber, L., 2015. Physicochemical properties of tadalafil solid dispersions–impact of polymer on the apparent solubility and dissolution rate of tadalafil. Eur. J. Pharm. Biopharm. 94, 106–115.

Woertz, C., Kleinebudde, P., 2015. Development of orodispersible polymer films with focus on the solid state characterization of crystalline loperamide. Eur. J. Pharm. Biopharm. 94, 52–63.

Yousaf, A.M., Kim, D.W., Oh, Y.K., Yong, C.S., Kim, J.O., Choi, H.G., 2015. Enhanced oral bioavailability of fenofibrate using polymeric nanoparticulated systems: physicochemical characterization and in vivo investigation. Int. J. Nanomedicine 10, 1819–1830.